Transactions of the 13th International Conference on Structural Mechanics in Reactor Technology (SMiRT 13), Escola de Engenharia - Universidade Federal do Rio Grande do Sul, Porto Alegre, Brazil, August 13-18, 1995

Spatial variation of earthquake ground motion based on dense array records

Nakamura, H., Yamazaki, F.
University of Tokyo, Tokyo, Japan

ABSTRACT: The spatial variation of earthquake ground motion in terms of the coherence function is examined based on twelve earthquake events observed at the Chiba array. A new coherence function model is proposed for space-time earthquake ground motion with consideration of previous research about the coherence function, assuming its limited portion to be homogeneous and stationary. A nonlinear regression analysis is conducted for estimating parameters of the coherence function model, and both the average and the variance are evaluated for the regression coefficients obtained from each event. The frequency-dependent correlation scale derived from the model is discussed. Finally, an application of the proposed model to earthquake events in Lotung, Taiwan, is presented.

1 INTRODUCTION

Even under the assumption that the free-field is a homogeneous soil medium, earthquake ground motion always varies in space. Two time histories of an array observation record will never coincide so long as the observation points differ (Katayama, 1991). It is usually the coherence function that describes the similarity of two time histories in frequency domain. Thus, the coherence function is utilized to characterize the spatial variation. Array observation records provide useful information for evaluating the spatial variation of ground motion during earthquakes. Quantifying the spatial variation for the response analysis of spatially extended structures is important. The spatial variation has been extensively studied by using coherence function based on the records of the SMART-1 array (e.g., Harada, 1984; Harichandran & Vanmarcke, 1986; Loh & Yeh, 1988; Sawada & Kameda, 1988; Hao et al., 1989), the LSST array (e.g., Kataoka et al., 1990; Abrahamson et al., 1991), and the Chiba array (e.g., Lu et al., 1994). Recently, coherence function has been developed for different soil types to study the effect of soil conditions based on records of several arrays (Somerville et al., 1991; Schneider et al., 1992). The objective of the present paper is to examine the spatial variation of free-field earthquake ground motion in terms of coherence function based on twelve earthquake events observed at the Chiba array, Japan.

2 ESTIMATE OF COHERENCE FUNCTION

Ground motions are vectorially converted into the radial and transverse directions. The coherence function of each of the three vibration components, i.e., radial (j=R), transverse (j=T), and up-down (j=U), is taken into account. In this study, the power spectra are computed by use of the limited portion of acceleration records assuming their strong motion parts to be homogeneous and stationary over the area and time duration considered. Coherence function is defined using spatial power spectrum, $P_{jj}(\xi_r, \xi_t, f)$, which depends on space coordinate (ξ_r, ξ_t) of separation vector and on frequency, f, converted from a time lag. Since only a limited portion of time histories is analyzed, the coherence function is obtained from the smoothed power spectra, $\hat{P}_{jj}(\xi_r, \xi_t, f)$, at specified locations, x and $x+\xi$, as

$$\gamma_{jj}(\xi_r, \xi_t, f) = \frac{\left|P_{jj}(\xi_r, \xi_t, f)\right|}{P_{jj}(0, 0, f)} \approx \frac{\left|\hat{P}_{jj}(\xi_r, \xi_t, f)\right|}{\sqrt{\hat{P}_{jj}(0, 0, f; x)\hat{P}_{jj}(0, 0, f; x+\xi)}} \quad \text{.....(1)}$$

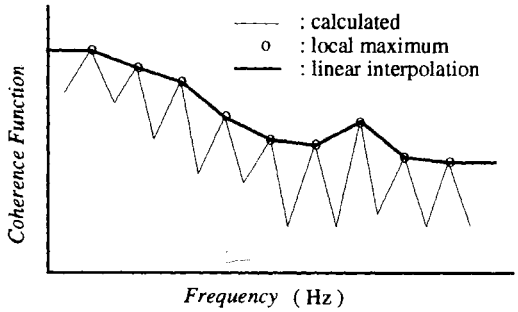

Fig. 1. Illustration of coherence function from a pair of acceleration records in frequency domain.

Table 1. *P*- and *S*-wave time window (in second, cf. Katayama et al., 1990) for each event used.

Event	*P-window*	*S-window*
8510	0.5~8.0	8.0~18.0
8519	2.0~9.5	11.0~21.0
8525	0.5~8.0	8.0~18.0
8601	0.5~8.0	9.0~19.0
8602	2.0~9.5	17.0~27.0
8722	0.5~8.0	8.0~18.0
8816	2.0~9.5	13.0~23.0
8823	2.0~9.5	11.0~21.0
9013	0.0~7.5	7.5~17.5
9014	0.0~7.5	7.5~17.5
9113	—	9.0~19.0
9202	0.5~8.0	12.0~22.0

The coherence function becomes unity for all frequency if the separation vector is zero:

$$\gamma_{jj}(0, 0, f) = 1.0 \quad (2)$$

As expected, coherence function decreases as both frequency and separation increase. It is shown, however, that especially at the dominant frequencies coherence function shows rapid decays only due to the rapid changes of phase spectrum (Lu et al., 1990). Therefore, the local decays are removed and the coherence function model is assumed to be an envelope of coherence function computed in the analysis following Kataoka et al. (1990). The peaks of the computed coherence function are picked up for that reason (Fig. 1).

Since the coherence function computed in the frequency domain depends strongly on the smoothing of power spectra, specifying the information of the smoothing procedure is important. A power spectrum is smoothed in the study by applying the Parzen's spectral window with a specified bandwidth of 0.4 Hz. The value of a specified bandwidth divided by the frequency increment must be larger than 560/151 (≈ 3.71) so that the truncation point is not beyond the folding point in the lag domain. As listed in Table 1, the time windows of 10 seconds for R and T, and 7.5 seconds for U are analyzed ($\Delta t = 0.005$ s). Zeros are padded at the end of the time history for a total of 10.24 seconds to compute the power spectrum. Thus, the minimum smoothing bandwidth is about 0.4 Hz in the analysis.

The peak values of the coherence function clearly decrease as the smoothing bandwidth increases. However, the number of peaks decreases at the same time. By using the relatively narrow smoothing bandwidth of 0.4 Hz, many peaks of the coherence function can be picked up, and the local decay also can be removed almost completely. Then, a nonlinear regression analysis to the peaks is conducted for estimating parameters of the model for the R, T, and U to investigate the difference of the value of model parameters among them. The authors believe that such a technique would yield an appropriate engineering estimate for coherence function.

Since coherence function gives us all information about horizontally spatial variation of earthquake ground motion, using a simple estimate that provides us with condensed information is convenient. The estimate is defined by the integral of coherence function over separation vectors as the frequency-dependent correlation scale (Vanmarcke, 1983) which is called correlation area in this study:

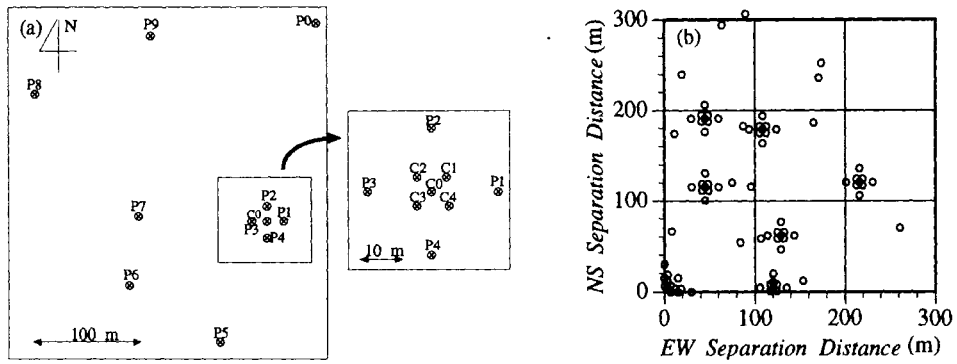

Fig. 2. (a) Layout of near surface (GL – 1 m) accelerometers and (b) distribution of separation vectors resulting from those 15 combinations.

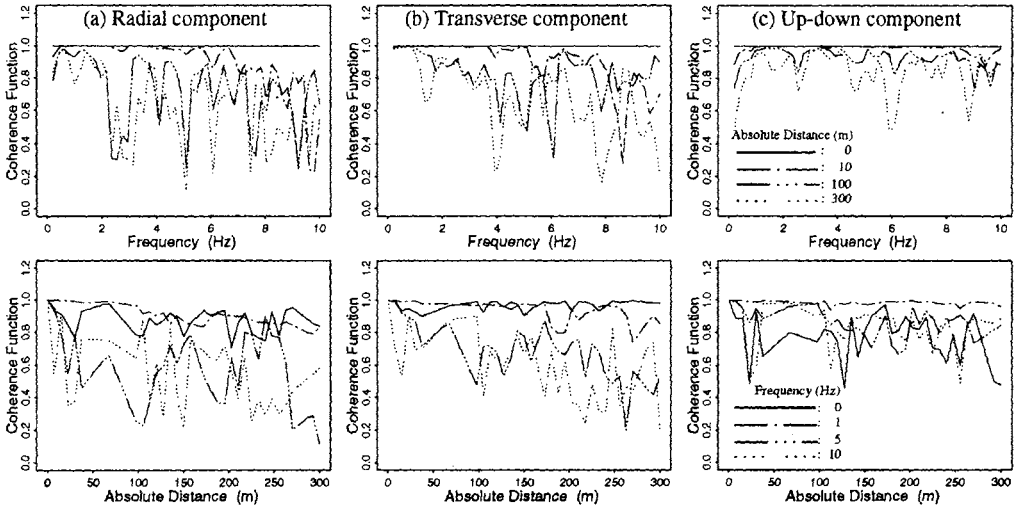

Fig. 3. Coherence function (event 9202) interpolated with respect to absolute distance (m); (a, b) for *S*-wave portion and (c) for *P*-wave potion (upper: frequency; lower: distance).

$$\theta_{jj}(f) = \iint_{\xi} \gamma_{jj}(\xi_r, \xi_t, f)\, d\xi_r d\xi_t \qquad (3)$$

3 CHIBA ARRAY RECORDS

In the array observation program at the Chiba site, fifteen accelerometers installed at GL – 1 m are covering an area of approximately 300 m square. The topographical and geological conditions in the site are generally simple and the ground surface is almost flat. Figure 2 shows the layout of the near surface (GL – 1 m) accelerometers and the distribution of separation vectors resulting from all combinations, for which the coherence function is linearly interpolated as a continuous surface for each event. Twelve earthquake events in Table 1 are analyzed using the records at GL – 1 m, in which the biggest ground motion record in the Chiba array database is event 8722. Though this event has records at only eleven locations, other eleven events have records at fifteen locations. The last four events are newly added to the original array database (Katayama et al., 1990). Calculating the *point* coherence function for all pairs of acceleration records, the coherence function can be plotted as a function of both frequency and separation by use of the spatial interpolation of the station spacing to be a limited set, e.g., as an example shown in Fig. 3 for the event 9202. The coherence function decreases with both frequency and separation. Similar results were obtained from the analysis of other events. Note that the distribution of the separation vectors available to estimate the coherence function may not be the same in different spatial ranges as can be seen from Fig. 2. Thus the confidence on each of the estimates could vary. In general, less confidence is associated with coherence function for large separations.

4 COHERENCE FUNCTION MODEL AT CHIBA SITE

Considering a preliminary analysis and previous works with respect to the coherence function, a Gaussian

Table 2. Regression coefficients averaged by those obtained from each event and those from all events using the coherence function model Eq. (4)

Event	Vibration component	Parameters of this coherence function model					Residual sum of squares	No. of data
		c_0 (sec)	c_1 (km/s)	c_2 (km/s)	c_3 (Hz)	c_4 (-)		
Average of each event	*Radial*	0.0302	74.5	0.0824	58.4	1.01		
	σ	0.0067	67.5	0.0136	41.9	0.16		
	Transverse	0.0310	41.2	0.0952	33.6	1.14		
	σ	0.0049	32.1	0.0226	23.4	0.22		
	Up-down	0.0069	8.9	0.1069	4.8	0.95		
	σ	0.0059	8.5	0.0297	11.7	0.19		
All events	*Radial*	0.0301	40.6	0.0799	44.2	0.95	226.3	19614
	Transverse	0.0302	32.0	0.0879	30.9	1.14	214.2	19718
	Up-down	0.0070	8.1	0.0986	5.2	0.87	65.7	16066

σ: standard deviation of 12 (*S*-window) or 11 (*P*-window) samples

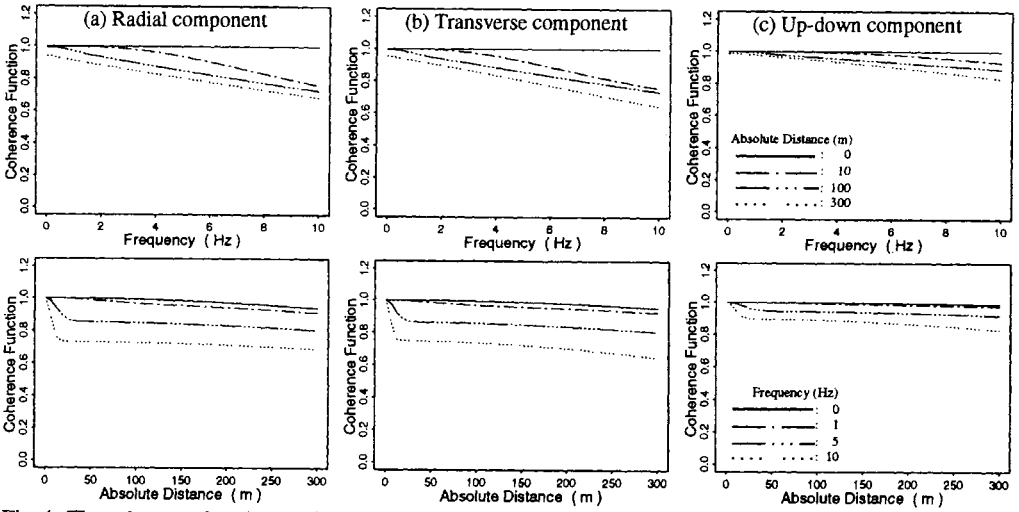

Fig. 4. The coherence function model, Eq. (4), with respect to frequency (Hz) and absolute distance (m) for *S*- and *P*-wave portion of event 9202 (cf. Fig. 3).

coherence function model with spatially ellipsoidal correlation structure is proposed for the spatial variation of space-time earthquake ground motion as follows:

$$\gamma_{jj}(\xi_r, \xi_t, f) = e^{-c_0 f} \exp\left\{-\frac{f^2 + {c_3}^2}{{c_1}^2}\left({c_4}^2 \xi_r^2 + \xi_t^2\right)\right\} + \left(1 - e^{-c_0 f}\right) \exp\left\{-\frac{f^2}{{c_2}^2}\left({c_4}^2 \xi_r^2 + \xi_t^2\right)\right\} \quad \text{.....(4)}$$

in which c_i's are parameters of the model. The parameter $c_0 f$ indicates decay with frequency at short distance and c_4 a degree of spatial anisotropy. Correlation area of each exponential is assumed as ${c_1}^2/\left(f^2 + {c_3}^2\right)$ for large distance and as ${c_2}^2/f^2$ for short distance.

The more the number of model parameters, the better estimations the model shows. Then, however, the evaluation as well as the regression analysis becomes difficult. Since adoption of the spatially quadratic exponential model could lead to considerable simplification of the subsequent mathematical manipulation, this model is assumed to describe the horizontally spatial correlation structure of the earthquake ground motion as double quadratic exponential function. A nonlinear least squares procedure is used to fit this model to the peaks of coherence function computed from the records for each event and for the lump sum of the twelve events. The result is listed in Table 2. Although the model considers the ellipsoidal correlation structure using the parameter c_4, it is found that the results of analysis do not show the significant anisotropic correlation structure of the coherence function model. The model for event 9202 is plotted for the *S*-wave portion of R and T, and for the *P*-wave portion of U in Fig. 4 that is corresponding to Fig. 3.

Both the average and the variance estimated are listed in Table 2, and evaluated for the regression coefficients obtained for each event. The C.O.V. for each parameter is plotted in Fig. 5. In particular, the parameter c_3 that has a dimension of frequency shows the largest variation for different earthquake events and controls the spatial correlation structure. The C.O.V. of the parameter is around 0.7. The parameters that vary mostly for each event have a dimension of frequency or distance. It is because space-time coher-

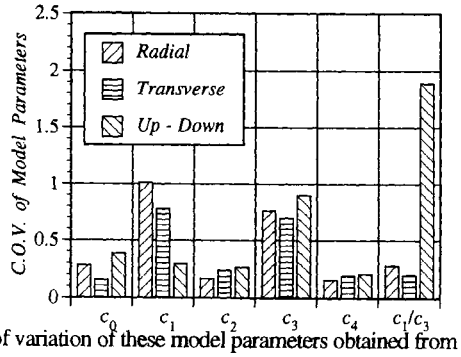

Fig. 5. Coefficient of variation of these model parameters obtained from each event (cf. Table 2).

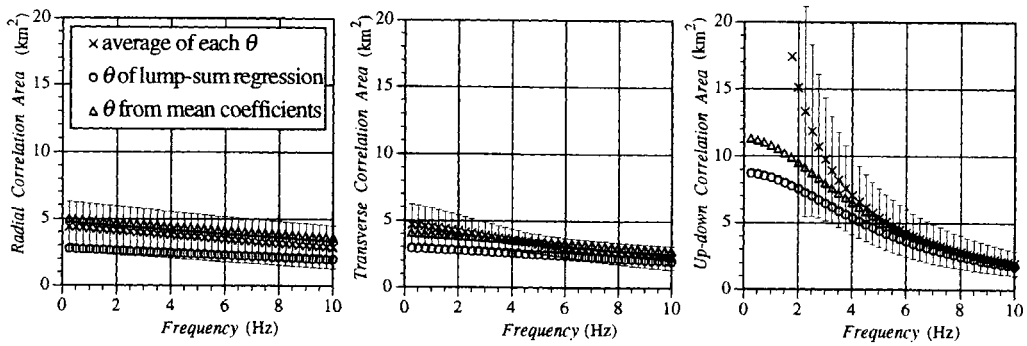

(a) Radial component (b) Transverse component (c) Up-down component

Fig. 6. Frequency-dependent correlation area (km^2); average of $\theta_{jj}(f)$ of each event (×) with ± 1 standard deviation; $\theta_{jj}(f)$ from lump-sum regression of all events (○); and $\theta_{jj}(f)$ from mean of regression coefficients of each event (△).

ence function changes by depending on frequency and distance and thus depends on the variable having the dimensions. In addition, the most largely varying parameters are included in the correlation area.

The frequency-dependent correlation area is derived from the coherence function model. After considering that the value of parameter c_2 is small compared with c_1, the correlation area is approximated as

$$\theta_{jj}(f) = 4\int_0^\infty \int_0^\infty \gamma_{jj}(\xi_r, \xi_t, f)\, d\xi_r d\xi_t = \frac{\pi}{c_4}\left\{ e^{-c_0 f} \frac{{c_1}^2}{f^2 + {c_3}^2} + \left(1 - e^{-c_0 f}\right)\frac{{c_2}^2}{f^2}\right\} \approx \frac{\pi}{c_4}\frac{(c_1/c_3)^2}{1+(f/c_3)^2} e^{-c_0 f} \quad (5)$$

Figure 6 shows the correlation area calculated in three ways. × indicates average of the area of each event with ± one standard deviation, ○ the area calculated from lump-sum regression of all events, and △ the area from mean of regression coefficients of each event. It is found by the analysis that the average of each of the areas is nearly equal to the areas determined from mean coefficients, while the areas determined from lump-sum regression are different from the other two. Although the correlation scale varies for each event because it includes the parameter c_3, the average value of the correlation scale shows that the correlation of U is higher than that of R and T.

5 APPLICATION OF THE MODEL TO LOTUNG ARRAY RECORDS

As an application of the proposed coherence function model, the array data obtained at the experiment site in Lotung, Taiwan, are also used for the analysis of spatial variation of earthquake ground motion. Note that

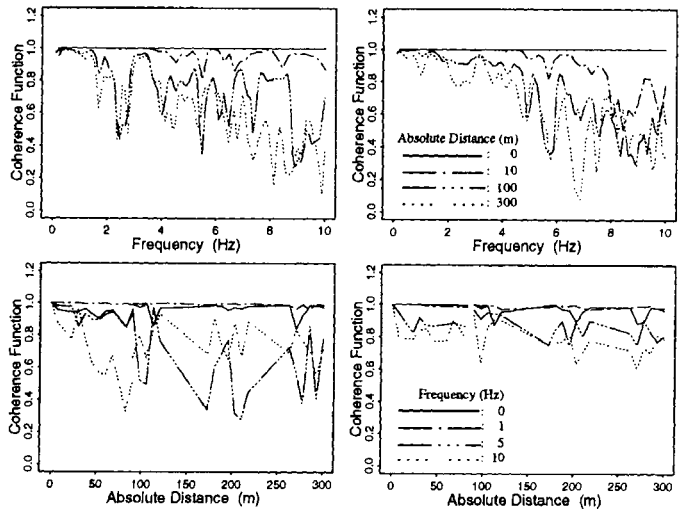

(a) A (SMART-1: No. 40; LSST: No. 7) (b) B (SMART-1: No. 45; LSST: No. 16)

Fig. 7. Coherence function (Transverse component of Lotung array records) interpolated with respect to absolute distance (m) for *S*-wave portion (upper: frequency; lower: distance).

a limited time duration of 10 seconds corresponding to the strong motion part of T is considered (SMART-1: $\Delta t = 0.01$ s, LSST: $\Delta t = 0.005$ s) in the analysis of the events A (May 20, 1986, $\Delta = 64$ km, $M_L = 6.5$; SMART-1: No. 40, LSST: No. 7) and B (November 14, 1986, $\Delta = 43$ km, $M_L = 7.0$; SMART-1: No. 45, LSST: No. 16). For the LSST array records, some station records close to the building and some faulty records were removed (e.g., Kataoka et al., 1990). The records collected in the inner ring are considered for the SMART-1 array in the same way as Hao et al. (1989). Then, only the records of stations spaced up to 400 m are used for regression analysis to compare the model parameters with those for the Chiba array.

Figure 7 shows the coherence function computed from both the records of the SMART-1 and the LSST array. Note that at a separation distance of around 100 m, there is a good agreement between the coherence function computed from the records of both these arrays. It can be seen that the coherence function for event A decreases with separation distance at high frequency of 5 and 10 Hz than that of event B. This is probably due to the difference of the magnitude. However, it cannot be concluded in the statistical sense, since the sample size may not be enough. The model parameters estimated from the records are; $c_0 = 0.0250$ s, $c_1 = 44.0$ km/s, $c_2 = 0.285$ km/s, $c_3 = 37.7$ Hz, $c_4 = 1.09$ for event A; and $c_0 = 0.0250$ s, $c_1 = 4.0$ km/s, $c_2 = 0.0473$ km/s, $c_3 = 1.1$ Hz, $c_4 = 1.07$ for event B. Although the coherence function model is not shown in a figure, comparison shows that the model envelops the computed coherence function quite well as in the case of the Chiba array. Finally, it is found that the correlation area of event B is very high at lower frequencies as, for example, that of U for *P*-wave window of the Chiba array, Fig. 6 (c). The correlation area of event A is almost the same as that of the Chiba array, Fig. 6 (b).

6 CONCLUSIONS

A new coherence function model that describes the spatial variation of earthquake ground motion over small areas is proposed. Both the average and the C.O.V. of the model parameters are obtained for all events from the peaks of the coherence function. Using a new model to represent the coherence function over small areas, it is demonstrated that the model parameters related to the correlation scale have a higher variance. An application of the proposed model is also presented to the combination of the coherence functions computed from both the SMART-1 and the LSST array records in Lotung, Taiwan. The coherence function model with the parameters estimated here could be utilized for the parametric study of response analysis in which spatially extended structures are considered.

REFERENCES

Abrahamson, N. A., J. F. Schneider & J. C. Stepp 1991. Empirical Spatial Coherency Functions for Application to Soil-Structure Interaction Analyses. *Earthquake Spectra*. 7: 1-27.

Hao, H., C. S. Oliveria & J. Penzien 1989. Multiple-Station Ground Motion Processing and Simulation Based on SMART-1 Array Data. *Nuclear Engineering and Design*. 111: 293-310.

Harada, T. 1984. Probabilistic Modeling of Spatial Variation of Strong Earthquake Ground Displacements. *Proc. 8th World Conf. on Earthquake Engineering*. II: 605-612.

Harichandran, R. S. & E. H. Vanmarcke 1986. Stochastic Variation of Earthquake Ground Motion in Space and Time. *Journal of Engineering Mechanics Division, Proc. ASCE*. 112: 154-174.

Kataoka, N., H. Morishita & A. Mita 1990. Spatial Variation of Seismic Ground Motion at Lotung Soil-Structure Interaction Experiment Site. *Proc. 8th Japan Earthquake Engineering Symposium*. 1: 607-612.

Katayama, T., F. Yamazaki, S. Nagata, L. Lu & T. Turker 1990. A Strong Motion Database for the Chiba Seismometer Array and its Engineering Analysis. *Earthquake Eng. Struct. Dyn.*. 19: 1089-1106.

Katayama, T. 1991. Use of Dense Array Data in the Determination of Engineering Properties of Strong Motions. *Structural Safety*. 10: 27-51.

Loh, C. H. & Y. T. Yeh 1988. Spatial Variation and Stochastic Modelling of Seismic Differential Ground Movement. *Earthquake Eng. Struct. Dyn.*. 16: 583-596.

Lu, L., F. Yamazaki & T. Katayama 1990. Soil Amplification Based on the Chiba Array Database. *Proc. 8th Japan Earthquake Engineering Symposium*. 1: 511-516.

Lu, L., T. Annaka, M. Shimada & M. Fujitani 1994. Analysis and Modeling of Spatial Coherence of Earthquake Ground Motions. *Proc. 4th U.S. National Conf. on Earthquake Engineering*. III: 199-208.

Sawada, T. & H. Kameda 1988. Modeling of Nonstationary Cross Spectrum for Multivariate Earthquake Motions by Multifilter Technique. *Proc. 9th World Conf. on Earthquake Engineering*. II: 795-800.

Schneider, J. F., N. A. Abrahamson & J. C. Stepp 1992. The Spatial Variation of Earthquake Ground Motion and Effects of Local Site Conditions. *Proc. 10th World Conf. on Earthquake Engineering*. 2: 967-972.

Somerville, P. G., J. P. McLaren, M. K. Sen & D. V. Helmberger 1991. Influence of Site Conditions on the Spatial Incoherence of Ground Motions. *Structural Safety*. 10: 1-13.

Vanmarcke, E. 1983. *Random Fields: Analysis and Synthesis*. MIT Press, Cambridge, MA.